Time-domain measurement of a self-amplified spontaneous emission free-electron laser with an energy-chirped electron beam and undulator tapering

G. Marcus,[1,a)] M. Artioli,[2] A. Bacci,[3] M. Bellaveglia,[3] E. Chiadroni,[3] A. Cianchi,[4] F. Ciocci,[2] M. Del Franco,[2] G. Di Pirro,[3] M. Ferrario,[3] D. Filippetto,[3] G. Gatti,[3] L. Giannessi,[2] M. Labat,[2,5] A. Mostacci,[6] A. Petralia,[2] V. Petrillo,[7] M. Quattromini,[2] J. V. Rau,[8] A. R. Rossi,[3] and J. B. Rosenzweig[1]

[1]*Particle Beam Physics Laboratory, Department of Physics and Astronomy, University of California Los Angeles, Los Angeles, California 90095, USA*
[2]*ENEA C.R. Frascati, Via E. Fermi, 45 00044 Frascati, RM, Italy*
[3]*INFN-LNF, Via E. Fermi, 40 00044 Frascati, RM, Italy*
[4]*INFN-Roma Tor Vergata & University of Rome Tor Vergata, Via della Ricerca Scientifica, 1-00133 Rome, Italy*
[5]*SOLEIL, L'Orme des Merisiers Saint-Aubin, BP 48 91192 GIF-sur-Yvette Cedex, France*
[6]*Università degli Studi di Roma La Sapienza, P.le Aldo Moro 5, 00185 Roma, Italy*
[7]*Università degli Studi di Milano and INFN-MI, Via Celoria, 16 20133 Milano, Italy*
[8]*ISM-CNR, Via del Fosso del Cavaliere, 100 00133 Roma, Italy*

(Received 25 June 2012; accepted 7 September 2012; published online 24 September 2012)

We report, with an unequivocal time-domain measurement, that an appropriately chosen undulator taper can compensate for an electron beam longitudinal energy-chirp in a free-electron laser amplifier, leading to the generation of single-spike radiation close to the Fourier limit. The measurements were taken using the frequency-resolved optical gating technique by employing an advanced transient-grating diagnostic geometry. The reconstructed longitudinal radiation characteristics are compared in detail to prediction from time-dependent three-dimensional simulations. © *2012 American Institute of Physics*. [http://dx.doi.org/10.1063/1.4754612]

Single pass x-ray, self-amplified spontaneous emission free-electron lasers (SASE FELs) can produce extremely bright, coherent, ultra-short radiation pulses.[1] These light sources have become an essential tool for investigating ultrafast chemical and physical processes, as they operate at spatial and temporal scales of atomic and molecular motion.[2–4] FELs operate on the principle that a coherent electromagnetic wave can be emitted and amplified many orders of magnitude by the collective beam-radiation instability that microbunches a relativistic electron beam (e-beam) as it propagates through a periodic static magnetic undulator. The narrow bandwidth radiation resulting from this interaction is peaked around the resonant frequency $\omega_r = 2\omega_u\gamma^2/(1 + K^2/2 + \gamma^2\theta^2)$, where $K = eB_u/m_0ck_u$ is the undulator strength parameter, $k_u = 2\pi/\lambda_u$ is the undulator wavenumber with undulator period λ_u, γ is the e-beam energy in units of the rest energy m_0c^2, and θ is the emission angle measured from the nominal beam propagation direction z. SASE FELs are only partially coherent, however, as the emitted light is the result of the amplification of initial incoherent radiation shot noise. Thus, the temporal structure of the light pulse is a collection of randomly distributed, short coherent spikes. Improving the coherence of SASE FEL light pulses has been the subject of much study,[5] with emphasis placed on producing a single longitudinally coherent radiation spike.[6–8]

One promising method to increase the radiation's longitudinal coherence relies on electron beam phase space manipulations that preferentially concentrate the gain along a small longitudinal portion of the e-beam. The method utilizes an energy-chirped e-beam and an appropriately chosen undulator taper (secular variation of the undulator field amplitude or period along z). This method is described in detail elsewhere,[9–11] but can be summarized as follows: The resonant amplified frequency in a FEL is determined by, among other things, the e-beam's mean energy (cf. ω_r, above). The amplified light propagates faster than the electrons as its group velocity during amplification remains larger than the e-beam velocity. In an energy-chirped e-beam, this velocity mismatch brings an amplifying radiation spike out of resonance as it slips forward in the beam frame, inhibiting the gain, unless an appropriate undulator taper (change in K) is applied to compensate for the local change in resonance. The undulator taper that provides this compensation is found to be $K(z) = 2\sqrt{(\gamma_s + \alpha z\eta\omega_u/\omega_r)^2\omega_u/\omega_r - 1/2}$, where γ_s is the normalized e-beam energy at the longitudinal position where the radiation spike begins amplification, α quantifies the energy chirp, and η is a factor that accounts for the different light propagation velocities in different stages of the amplification process, e.g., exponential gain or saturation.[10] For a short electron beam,[6] it is possible for only one coherent radiation spike undergoing exponential gain and propagating at the appropriate velocity to match the e-beam energy chirp and associated undulator taper; this spike eventually reaches saturation.

Observation of this phenomenon is not possible at x-ray wavelengths because of the lack of appropriate diagnostics. Thus one must examine, as is often the case in FEL research,

a)Author to whom correspondence should be addressed. Electronic mail: gmarcus@physics.ucla.edu.

the physics of this scheme at longer wavelengths. In this regard, the frequency-resolved optical gating[12] (FROG) diagnostic and pulse reconstruction technique has proven to be effective in analyzing ultra-fast light sources in the optical and near-infrared wavelength regions. In this letter, we report a time-domain measurements of near single-spike radiation produced from a single pass SASE FEL amplifier operating under the e-beam energy chirp and undulator tapering conditions discussed above, by utilizing an advanced transient-grating (TG) FROG diagnostic. We compare these results with fully three-dimensional time dependent numerical simulations obtained from the code GENESIS.[13]

The experiment, with e-beam energy chirp and compensating undulator taper, was conducted at the SPARC (Sorgente Pulsata Auto-amplificata di Radiazione Coerente) FEL Facility in Frascati.[14] High brightness electron beams are created at SPARC using an injector consisting of a 1.6 cell rf photocathode gun, followed by three traveling wave linac sections, two of which are embedded in focusing solenoids. Longitudinal e-beam compression is obtained by running the first linac section off crest near the zero-crossing phase, where the first solenoid is used to optimize emittance compensation.[15] This method, termed velocity bunching,[16] gives an increase in the peak current while leaving a residual energy chirp in the electron beam longitudinal phase space.[17,18] Two quadrupole triplets along with a dipole based magnetic spectrometer and RF deflecting cavity allow measurement of time-projected and time-resolved (slice) e-beam parameters, which are summarized in Table I. Transport optics match the beam into the undulator, which is comprised 6 independent, variable gap sections. The undulator sections were discretely tapered through gap adjustment in accord with the above prescription for $K(z)$, and for a radiation spike propagating with group velocity near the speed of light. After undergoing exponential gain and entering saturation (see Table I for relevant parameters), the FEL light exiting the last undulator section was directed to a diagnostic station where it was input to the FROG device.

The TG FROG diagnostic used to extract the longitudinal profile was constructed with the unique capabilities and challenges of measuring FEL output in mind,[19] particularly in its extendibility to shorter wavelength operation. It was based on a geometry initially proposed and demonstrated by Lee *et al.*[20] The diagnostic geometry as constructed is shown in Fig. 1. The expression for the FROG trace for this particular geometry is $I^{TG}_{FROG}(\omega,\tau) \propto \left|\int_{-\infty}^{\infty} E(t)|E(t-\tau)|^2 \exp(-i\omega t)\,dt\right|^2$. Iterative Fourier transform algorithms are used to retrieve the complex electric field, $E(t)$. While the TG FROG concept has previously been studied,[21,22] it was not used in the FEL context. Here, we emphasize that the geometry implemented has minimal alignment degrees of freedom and operates on a single-shot basis; these key features help simplify complex measurements at a FEL.

TABLE I. Experimental e-beam, undulator, and radiation parameters.

Parameter	Symbol	Value
Charge	Q	250 pC
Peak current	I	264 A
Mean e-beam energy	E	113.1 MeV
e-beam energy chirp	α	$-2.5\,\mathrm{keV}/\mu\mathrm{m}$
rms slice energy spread	σ_γ	5×10^{-3}
Norm. x(y) emittance	$\epsilon_{n,x(y)}$	2.3(1.6) mm mrad
Ave. x(y) beta function	$\beta_{x(y)}$	1.5 m
Undulator period	λ_u	2.8 cm
Undulator parameter	K	1.31
Radiation wavelength	λ	530 nm
Max. radiation energy	E_r	31.5 μJ
Measured gain length	L_g	92 cm

At this point, it is useful to discuss relevant previous experimental results in chirped SASE FELs and the applications of FROG diagnostics to provide context for our results. Andonian *et al.*[23] studied the effects of a chirped e-beam on the spectral characteristics of the output radiation and found the resulting light exhibited an anomalously large bandwidth. Li *et al.*[24] used a negatively chirped e-beam, where the electrons in the head of the bunch had a higher energy than that of the electrons in the tail, to compensate for the light's intrinsic positive chirp that naturally arises from the SASE process. Velocity bunching, however, results in a positively chirped electron beam, which serves to reinforce this intrinsic chirp. In the present experiment, the undulator tapering serves to compensate for both the intrinsic SASE chirp as well as the e-beam chirp, while simultaneously compensating for the electron energy loss to the FEL radiation. This

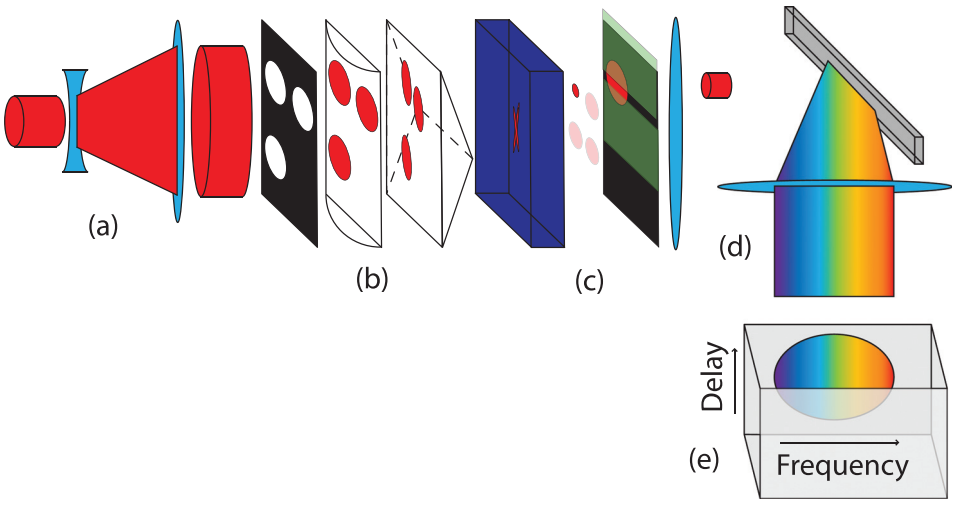

FIG. 1. Schematic of transient-grating FROG diagnostic: (a) beam expander; (b) input mask, cylindrical lens, Fresnel biprism; (c) nonlinear optical medium, output mask, knife edge slit; (d) focusing optics, diffraction grating; (e) CCD camera.

scheme effectively preserves the narrowband radiation nominally produced in a standard non-chirped single-spike SASE FEL as seen in Ref. 10. However, it should be noted that no direct time-domain measurement had been achieved in Ref. 10 and the pulse length at the Fourier limit was only estimated from the spectral width. The TG FROG was thus implemented as an advanced diagnostic that could simultaneously perform the measurements, while pushing the diagnostic paradigm to shorter wavelength operation. Undulator tapering has also been studied previously in the context of seeded FELs by Wang *et al.*,[25] where significant efficiency enhancement and spectral narrowing were observed. The present experiment, however, uses an undulator taper in a SASE FEL to suppress radiation growth where the change in resonance due to slippage is not compensated by an e-beam energy chirp. Superradiant FEL pulses generated by a coherent seed, such as those observed with a SHG FROG by Watanabe *et al.*[26] also share many similar characteristics to single-spike SASE pulses. The physical mechanisms that govern their growth and propagation, however, are different than those at play here. Finally, we note that use of TG FROG, introduced here for a FEL, unambiguously yields the direction of time.

A typical experimental FROG trace is shown in Fig. 2(a); note that there is notable noise in the image. One strength of the reconstruction process, however, is the ability of the algorithm to filter out the noise because of the robust over-sampling involved.[27] The reconstructed trace, Fig. 2(b), shows excellent overall agreement with the experimental trace. These results are compared to fully time-dependent, 3D particle-based simulations using GENESIS. Here, the experimentally measured e-beam parameters from Table I were used to specify the input particle distribution. Post-processing the simulation data with an algorithm to extract the light's longitudinal profile at the transverse location indicated by the input mask in Fig. 1 results in the simulated FROG trace found in Fig. 2(c). The agreement in the details of the reconstructed and simulated FROG traces is striking. There are several distinct features which are well reproduced by the simulated FROG trace, such as the asymmetry in the main body, indicating a slight chirp, as well as the length and shape of the leading and trailing tails. This agreement extends to the reconstructed and simulated longitudinal profiles found in Figs. 3(a) and 3(b). The reconstructed longitudinal profile is composed of a dominant coherent spike with a full width at half maximum (FWHM) of $\delta\tau^R_{FWHM} = 98$ fs followed by a weaker trailing tail. The same signature can be found in the simulated results where the single dominant coherent spike has a FWHM of $\delta\tau^G_{FWHM} = 91$fs. It is interesting to note that there remains a small positive chirp in the phase in both profiles that is likely a result of the discrete nature of the tapering.

One advantage of using the FROG technique is that the temporal and spectral content along with the pulse's phase information can be extracted simultaneously from the associated trace. This allows a rigorous determination of the time-bandwidth product (TBP),[28] $TBP = \tau_{rms}\omega_{rms}$, where $\omega^2_{rms} = \int_{-\infty}^{\infty} E'(t)^2 dt + \int_{-\infty}^{\infty} E(t)^2\phi'(t)^2 dt$. Here, $E(t) = \sqrt{I(t)}$ is the electric field's real amplitude, $\phi(t)$ is the temporal phase minus the mean frequency, the prime indicates differentiation with respect to time, and the intensity, $I(t) = |E(t)|^2$, is normalized to have unity time integral. This expression for the rms bandwidth contains contributions from variations in pulse amplitude as well as those due to phase changes. A

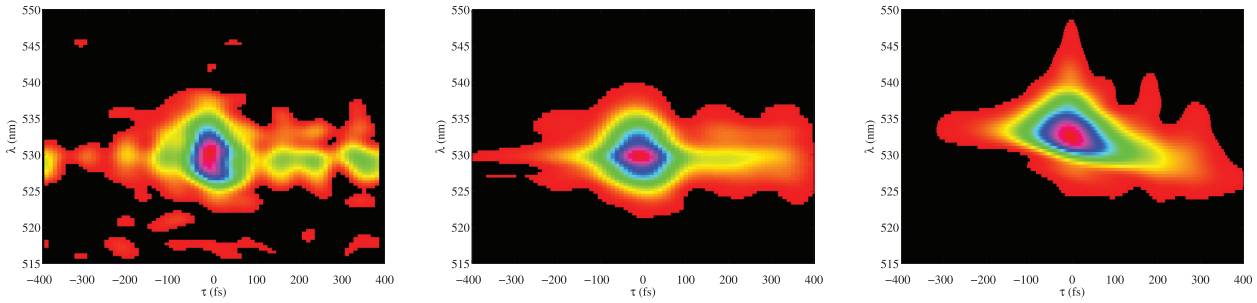

(a) Experimental FROG Trace (b) Reconstructed FROG Trace (c) GENESIS FROG Trace

FIG. 2. Comparison of the (a) experimental, (b) reconstructed, and (c) simulated FROG traces.

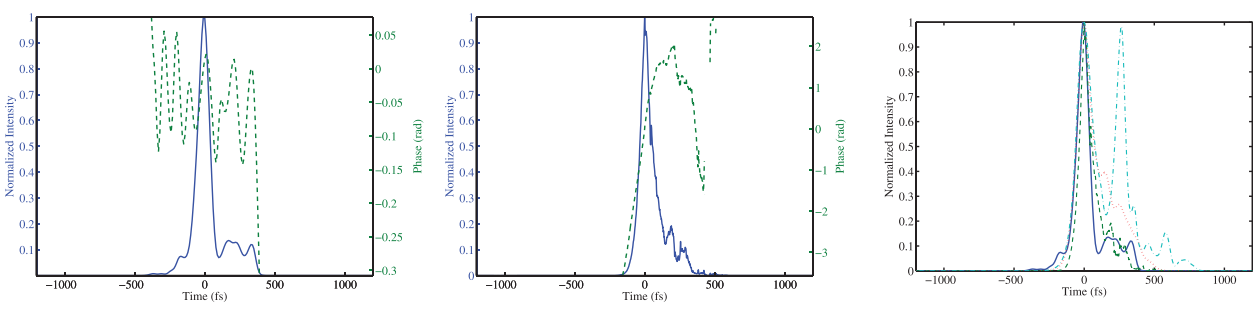

(a) (b) (c)

FIG. 3. Normalized longitudinal profiles from the (a) reconstruction and (b) simulation. (c) Comparison between the reconstructed intensity (solid-blue), simulated power at the mask (dashed-green), total pulse simulated power (dotted-red), and total pulse simulated power in the absence of an undulator taper (dotted/dashed-turquoise).

similar relationship holds for τ^2_{rms}. For the pulse in Fig. 3(a), we have $TBP \sim 1.2$. This is highly significant, indicating that single-spike radiation production was nearly achieved while operating in the chirp and taper scenario.

One concern inherent with use of the TG FROG on a FEL is that the on axis light is discarded by the input mask. Fig. 3(c) compares the off-axis and total power from the reconstructed and simulated data. While the full power profile shows a more pronounced tail, the main features of the pulse are still captured by the off axis data gathered by the FROG system. Fig. 3(c) also shows the full power profile for an identical simulation in the absence of an undulator taper to emphasize the utility of the tapering. Multiple radiation spikes are clearly evident. The subtlety of interpreting the results from the TG FROG is an inherent challenge in FELs (as opposed to standard lasers), due to their non-negligible spatial chirp. Nevertheless, the current measurement is seen to be robust.

This research is supported by grants from US DOE Contract Nos. DE-FG02-07ER46272 and DE-FG03-92ER40693, Office of Naval Research Contract No. N00014-06-1-0925, and DARPA Contract No. N66001-11-4197.

[1]P. Emma, R. Akre, J. Arthur, R. Bionta, C. Bostedt, J. Bozek, A. Brachmann, P. Bucksbaum, R. Coffee, F. J. Decker *et al.*, Nature Photon. **4**, 641 (2010).
[2]J. Marangos, Contemp. Phys. **52**, 551 (2011).
[3]C. M. Gunther, B. Pfau, R. Mitzner, B. Siemer, S. Roling, H. Zacharias, O. Kutz, I. Rudolph, D. Schondelmaier, R. Treusch *et al.*, Nature Photon. **5**, 99 (2011).
[4]R. Neutze, R. Wouts, D. van der Spoel, E. Weckert, and J. Hajdu, Nature **406**, 752 (2000).
[5]E. Saldin, E. Schneidmiller, and M. Yurkov, Opt. Commun. **202**, 169 (2002).
[6]R. Bonifacio, L. De Salvo, P. Pierini, N. Piovella, and C. Pellegrini, Phys. Rev. Lett. **73**, 70 (1994).
[7]J. Rosenzweig, D. Alesini, G. Andonian, M. Boscolo, M. Dunning, L. Faillace, M. Ferrario, A. Fukusawa, L. Giannessi, E. Hemsing *et al.*, Nucl. Instrum. Methods Phys. Res. A **593**, 39 (2008).
[8]J. Feldhaus, E. Saldin, J. Schneider, E. Schneidmiller, and M. Yurkov, Opt. Commun. **140**, 341 (1997).
[9]E. L. Saldin, E. A. Schneidmiller, and M. V. Yurkov, Phys. Rev. ST Accel. Beams **9**, 050702 (2006).
[10]L. Giannessi, A. Bacci, M. Bellaveglia, F. Briquez, M. Castellano, E. Chiadroni, A. Cianchi, F. Ciocci, M. E. Couprie, L. Cultrera *et al.*, Phys. Rev. Lett. **106**, 144801 (2011).
[11]G. Dattoli, L. Giannessi, S. Pagnutti, and P. Ottaviani, Opt. Commun. **285**, 710 (2012).
[12]R. Trebino and D. J. Kane, J. Opt. Soc. Am. A **10**, 1101 (1993).
[13]S. Reiche, Nucl. Instrum. Methods Phys. Res. A **429**, 243 (1999).
[14]L. Giannessi, D. Alesini, P. Antici, A. Bacci, M. Bellaveglia, R. Boni, M. Boscolo, F. Briquez, M. Castellano, L. Catani *et al.*, Phys. Rev. ST Accel. Beams **14**, 060712 (2011).
[15]M. Ferrario, D. Alesini, A. Bacci, M. Bellaveglia, R. Boni, M. Boscolo, M. Castellano, E. Chiadroni, A. Cianchi, L. Cultrera *et al.*, Phys. Rev. Lett. **104**, 054801 (2010).
[16]L. Serafini and M. Ferrario, AIP Conf. Proc. **581**, 87 (2001).
[17]S. G. Anderson, P. Musumeci, J. B. Rosenzweig, W. J. Brown, R. J. England, M. Ferrario, J. S. Jacob, M. C. Thompson, G. Travish, A. M. Tremaine *et al.*, Phys. Rev. ST Accel. Beams **8**, 014401 (2005).
[18]D. Filippetto, M. Bellaveglia, M. Castellano, E. Chiadroni, L. Cultrera, G. Di Pirro, M. Ferrario, L. Ficcadenti, A. Gallo, G. Gatti *et al.*, Phys. Rev. ST Accel. Beams **14**, 092804 (2011).
[19]G. Marcus, G. Andonian, M. Ferrario, A. Fukusawa, L. Giannessi, P. Musumeci, L. Palumbo, S. Reiche, and J. Rosenzweig, in Proceedings of the 23rd Particle Accelerator Conference, Vancouver, Canada, 2009.
[20]D. Lee, S. Akturk, P. Gabolde, and R. Trebino, Opt. Express **15**, 760 (2007).
[21]J. N. Sweetser, D. N. Fittinghoff, and R. Trebino, Opt. Lett. **22**, 519 (1997).
[22]M. Li, J. P. Nibarger, C. Guo, and G. N. Gibson, Appl. Opt. **38**, 5250 (1999).
[23]G. Andonian, A. Murokh, J. B. Rosenzweig, R. Agustsson, M. Babzien, I. Ben-Zvi, P. Frigola, J. Y. Huang, L. Palumbo, C. Pellegrini *et al.*, Phys. Rev. Lett. **95**, 054801 (2005).
[24]Y. Li, J. Lewellen, Z. Huang, V. Sajaev, and S. V. Milton, Phys. Rev. Lett. **89**, 234801 (2002).
[25]X. J. Wang, H. P. Freund, D. Harder, W. H. Miner, J. B. Murphy, H. Qian, Y. Shen, and X. Yang, Phys. Rev. Lett. **103**, 154801 (2009).
[26]T. Watanabe, X. J. Wang, J. B. Murphy, J. Rose, Y. Shen, T. Tsang, L. Giannessi, P. Musumeci, and S. Reiche, Phys. Rev. Lett. **98**, 034802 (2007).
[27]D. N. Fittinghoff, K. W. DeLong, R. Trebino, and C. L. Ladera, J. Opt. Soc. Am. B **12**, 1955 (1995).
[28]L. Cohen, *Time-Frequency Analysis*, Prentice Hall Signal Processing Series (Prentice-Hall PTR, 1995).